Key Engineering Materials
ISSN: 1662-9795, Vol. 1050, pp 93-102
doi:10.4028/p-kJ2Cti

Submitted: 2026-01-18
Revised: 2026-02-25
Accepted: 2026-02-26
Online: 2026-04-16

AI-Based Predictions of Forming Effects for Enhanced Crash Simulation

Ingolf Lepenies

SCALE GmbH, Pohlandstraße 19, 01309 Dresden, Germany
ingolf.lepenies@scale.eu

Keywords: Deep Drawing, Physics-Informed AI, Forming Effects, Virtual Vehicle Development

Abstract. In the early concept phase of vehicle development, crash simulations must provide reliable statements on energy absorption and failure behavior, although detailed forming simulations and process data are typically not yet available. Manufacturing-induced material states, such as plastic pre-strains and local sheet thickness distributions, are therefore often neglected or approximated using simplified low-fidelity approaches with high uncertainty. This contribution introduces UmMatCraML, a data-driven medium-fidelity method for rapid initialization of typical crash shell meshes (element edge lengths 3–5 mm) with forming-induced field variables. Starting from the final component geometry, a purely geometric unfolding is performed to approximate the blank, from which a mesh- and coordinate-independent areal strain A_r is determined. A monotonicity-preserving gradient boosting regressor subsequently compensates for systematic deviations of this geometric surrogate model compared to high-fidelity deep drawing simulations, with four Hockett-Sherby parameters consistently parameterizing the material description. The training data are generated from approximately 5,000 LS-DYNA forming simulations and cover a broadly varied, physically consistent parameter space. In validation on a demonstrator part, UmMatCraML reduces the computation time for determining forming-induced component properties from about 60 min for High-Fidelity-Simulation (HFS) or 10–15 min for Low-Fidelity-Simulation (LFS) to under 10 s, with simultaneously improved prediction quality. Demonstrations on components of a Toyota Yaris full-vehicle model show robust predictions even with trimming and perforations. Limitations arise from the model assumptions made (e.g., isotropic hardening, limited mapping of multi-stage process paths). Overall, UmMatCraML enables real-time, reproducible provision of manufacturing-induced field variables for concept crash simulations without explicit tool modeling.

1. Introduction

In the early concept phase of vehicle development, the crash properties of the full vehicle must be estimated. The prediction of structural behavior depends significantly on locally varying material states arising from the forming process. These properties, particularly plastic pre-strains and sheet thinning, influence energy absorption and failure behavior.

Crash simulations as dynamic structural analyses and forming simulations are both used early in component development but differ in temporal positioning, modeling detail, and objectives [10]. Forming simulations primarily serve to ensure manufacturability and process design, while crash simulations evaluate structural energy absorption capacity. Consistent coupling of both domains is required to consider manufacturing-induced properties in crash models. In industrial practice, this mapping typically occurs only in late series phases, sporadically and with idealized material models.

Finite element-based forming simulations represent the state of the art for mapping complex sheet forming processes [1]. They are based on nonlinear, anisotropic, and plastic material models that consistently capture direction-dependent yield stress, plastic hardening, and stress- and strain-dependent material responses [13, 14]. Extended multiphysical approaches couple mechanical and thermal fields and allow an integrated description of friction, temperature development, and the resulting stress states during the forming process.

In early development stages, manufacturing-induced properties are often neglected. Reasons include the high computational effort of detailed finite element forming simulations (high-fidelity simulations, HFS) with element sizes of approximately 1 mm and the lack of valid forming data with

incomplete geometries. Simplified one-step simulations (low-fidelity simulations, LFS) with element sizes of 3–5 mm and two-parameter hardening laws provide initial estimates but are inaccurate due to coarse geometry approximations and simplified material descriptions [12]. Additionally, there is a significant discretization difference between forming simulations with fine meshes and crash simulations, which typically use element edge lengths of 3–5 mm. Reconstructing an initial blank from a trimmed final geometry with perforations, beads, and flanges poses an inverse and ill-posed problem under these boundary conditions.

Recent research has investigated data-driven methods to accelerate forming simulations and predict forming outcomes. Surrogate models, neural networks, and gradient boosting approaches have been applied to predict thinning and strain fields. However, many approaches remain limited to simplified geometries or narrow process windows, require dense input data, or lack physical constraints, which can lead to non-plausible predictions when extrapolating to new components [2, 3].

Research gap. In the early concept phase, the assessment of crash properties primarily requires the dominant forming-induced plastic deformations and sheet-thinning extrema. Accordingly, there is a need for a coordinate-independent, mesh-based method that provides physically plausible thickness and plastic strain fields directly on crash FE meshes without explicit tool modeling and without the computational effort of HFS, while significantly improving the systematic inaccuracies of LFS for complex, trimmed and perforated geometries. In this context, effects that are typically second-order for early-phase crash assessment – such as material anisotropy and kinematic hardening – can be intentionally neglected to enable robust, fast predictions. Moreover, the explicit consideration of multi-stage forming is not required for methods targeting early-phase concept assessment.

2. Methodology and Procedure

The UmMatCraML approach addresses the performant provision of manufacturing-induced component properties for crash-relevant simulations in early development phases. The objective is to identify and quantify regions of large plastic deformations and crash-relevant sheet-thinning extrema in the component. Training data from low-fidelity forming simulations (one-step-simulations without tools) are used to learn the systematic deviations between the geometric surrogate and physics-based results, enabling a performant and sufficiently accurate one-step methodology. The target is to deliver results significantly faster than established FEM-based one-step solvers. Non-objectives are the prediction of springback, wrinkling, and anisotropic material behavior including kinematic hardening, which are explicitly not addressed within the proposed scope.

The approach follows a simplified inverse procedure conceptually related to one-step solvers. Starting from the final component geometry, the initial blank is approximated by purely geometric unfolding of the three-dimensional surface into the plane. The unfolding is implemented as a conformal surface-to-plane mapping that preserves local angles and maps a three-dimensional surface with spatially varying thickness to a two-dimensional representation with constant thickness, while minimizing global volume changes to maintain volume constancy. Local deformation measures are derived by comparing deformed and undeformed element areas under the assumption of volume constancy; plastic material behavior and process-related effects are not modeled during unfolding.

Training data from low fidelity forming simulations (LFS) are used to learn the systematic deviations between the geometric surrogate and physics-based results. The goal is to identify and quantify regions with large plastic deformations and crash-relevant sheet-thinning extrema; springback, wrinkling, and anisotropic material behavior with kinematic hardening are explicitly not addressed. Within these scope assumptions, a performant and sufficiently accurate one-step methodology is targeted for early-phase crash assessment.

The starting point is a shell FE mesh of the final component geometry (element sizes 3–5 mm, including holes, trimming, and flanges). Fig. 1 shows the underlying workflow. In process step I, the post-forming 3D geometry without holes is derived. This is geometrically unfolded into the plane

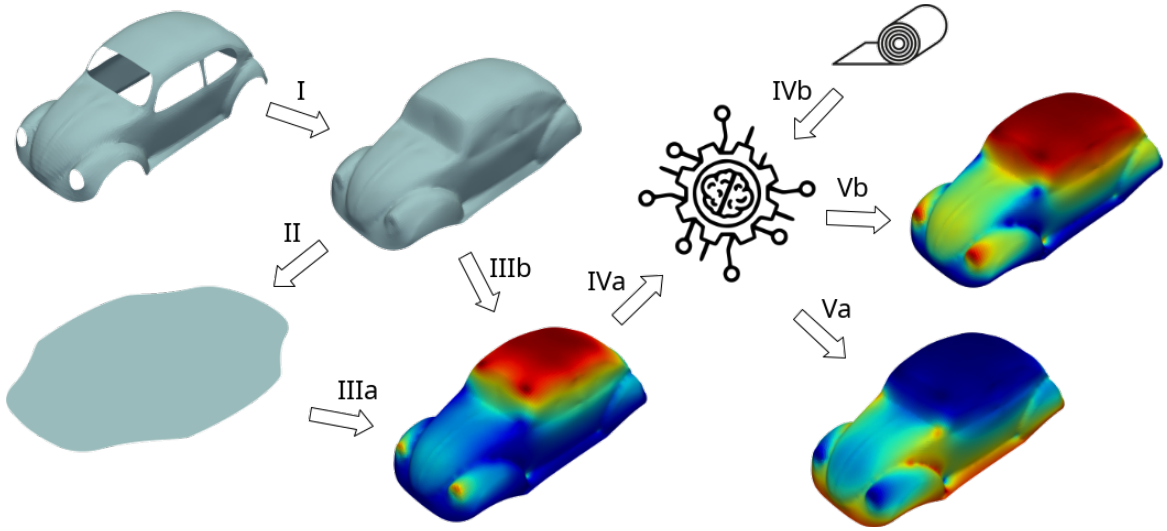

Fig. 1: The UmMatCraML Workflow: I - Hole-filling of the 3d-mesh, II - unfolding of the 3d-mesh in 2d-mesh, III - calculation of strain measure $A_{\mathrm{r,\,uvmap}}$, IV - AI prediction of strain measure $A_{\mathrm{r,real}}$, V - calculation of sheet thickness and plastic strain based on $A_{\mathrm{r,\,real}}$

in process step II to approximate the initial blank. Based on the area comparison, the areal strain $A_r = A/A_0$ is calculated in steps IIIa and IIIb:

with A0 as the undeformed and A as the deformed element area. The method ensures volume constancy but does not consider plastic material behavior or process-related effects (friction, tool contact, multi-stage forming).

The systematic deviations of this geometric surrogate model prediction compared to low- and high-fidelity forming simulationresults (HFS) are compensated by the UmMatCraML model.

Training and validation data are systematically generated from numerical deep drawing processes under defined process parameters, material models, and boundary conditions. Target variables are plastic strains and local sheet thinning, as these significantly influence failure and energy absorption behavior in crash analyses.

The feature representation via the areal strain Ar is designed to be mesh-independent to enable generalization to unknown discretizations. The vector Ar serves here as the sole geometric input vector for the AI model (step IVa). Notably, this is a coordinate-independent description of the geometry.

Additionally, material-describing features are integrated (step IVb). In accordance with the parsimony principle of science, the functional relationship is modeled by exactly four parameters: the four Hockett-Sherby parameters of the hardening curve, cf. Fig. 4.

In step V, inference occurs with the 5 input parameters: The model predicts sheet thicknesses and plastic strains. These are mapped onto the original crash model in steps VIa and VIb, allowing manufacturing-induced effects to be consistently incorporated into the structural dynamic analysis.

The method was prototypically implemented in a prediction tool. Validation was based on the Kirchhoff Automotive demonstration LS-Dyna model [7], which served as a reference high-fidelity model (HFS) – a LS-DYNA model with die, punch and holder – for comparing predicted and model-based system states. The agreement of the results was evaluated using quantitative metrics, verifying the functional correctness of the implementation and the consistency of the methodological assumptions.

2.1 AI-compliant geometry description

Step I (cf. Fig. 1) serves to generate the post-forming 3D geometry and forms the basis for the subsequent blank determination. Several methodological approaches are considered for estimating the blank. These include using the original contour of the crash mesh, optionally with or without considering existing perforations, a radial offset to determine a concave hull contour, or alternatively

determining a convex hull contour. Based on the selected contour definition, an automatic mesh generation is performed, from which the initial blank geometries are derived, cf. Fig. 2. The subsequent unfolding of the three-dimensional geometry into the plane is based on geometric algorithms that provide the blank approximation.

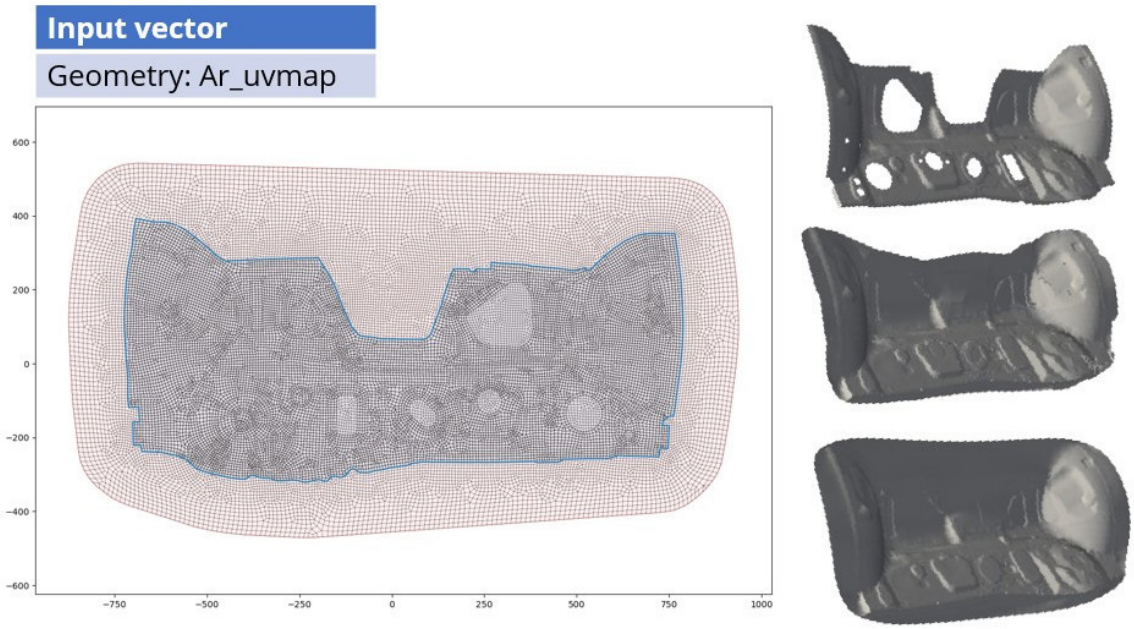

Fig. 2: Preprocessing: FE Model Extraction and Approximation of the Sheet Blank

To ensure efficient, consistent, and traceable processing of the data generated, the data management system SCALE.sdm is used (cf. Fig. 3). The system handles the structured capture, storage, and versioning of data as well as the control of associated processing workflows, thus providing a reproducible data basis for downstream analysis and evaluation steps.

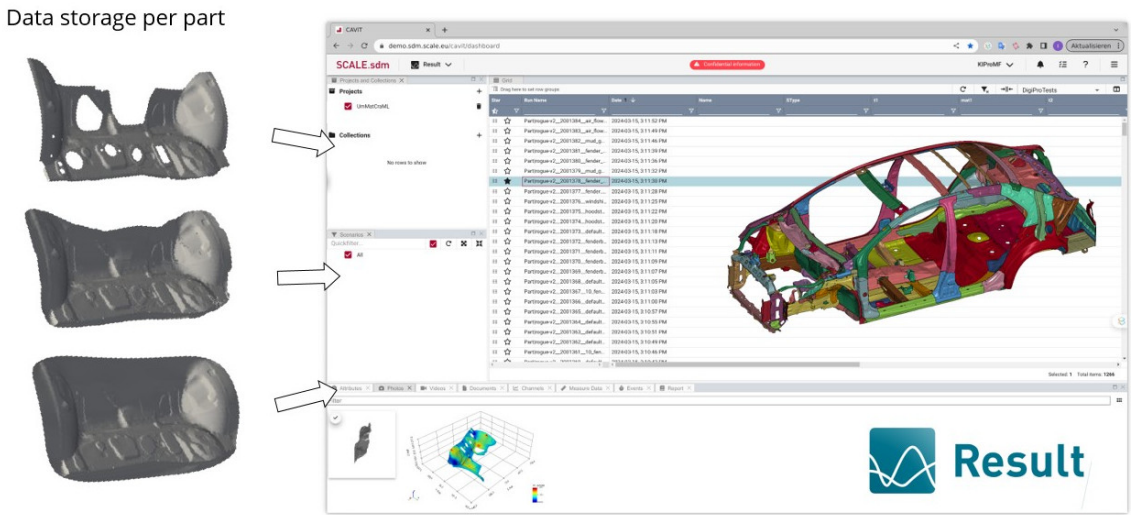

Fig. 3: Data Management in SCALE.sdm

2.2 AI-compliant material Description

All materials used are consistently described in the UmMatCraML model by a uniform set of Hockett-Sherby hardening parameters [4]. Thus, the same phenomenological hardening law is assumed for all materials, whereby material-specific differences are mapped exclusively via the parametric expression of the model and not via different model approaches.

The Hockett-Sherby model describes the isotropic hardening behavior of metallic materials under plastic deformation. The model parameterizes the flow curve via the initial yield stress σ_0 as well as the saturation stress $\sigma_{a,true}$ and additionally considers the Considère stress σ_c and the associated Considère strain ε_c. These quantities characterize the transition from homogeneous plastic deformation to material instability due to diffuse necking. By explicitly incorporating the instability criteria, the model formulation allows consistent mapping of the hardening behavior up to the uniform strain.

Fig. 4 shows an exemplary parameter identification for the dual-phase steel DP980. The model parameters were determined by fitting to experimental stress-strain data. The model captures the characteristic decrease in hardening rate for steels with increasing plastic strain and allows consistent consideration of material instability. The parameterization is reproducible, as the used model form, number of degrees of freedom, and underlying assumptions are clearly defined. Limitations of the approach arise from the assumption of isotropic hardening, whereby direction-dependent effects and kinematic components are not mapped.

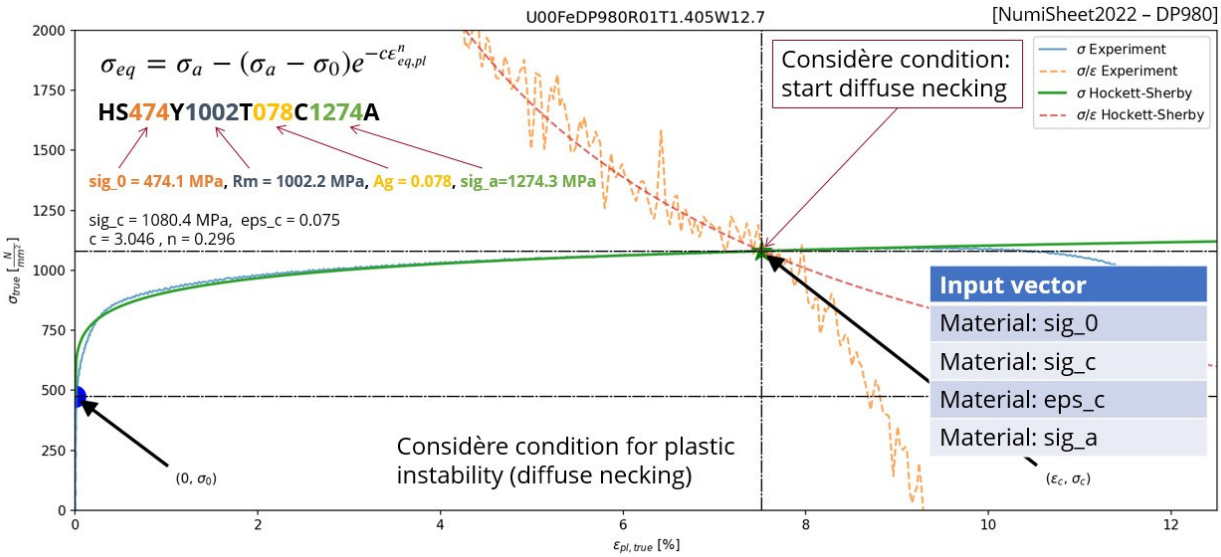

Fig. 4: Approximation of the hardening behavior of metallic materials considering material instability.

The material behavior can be generically generated. For this, a naming scheme was developed. Exemplarily, the designation HS450Y659T139C900A describes a material with a technical yield stress $\sigma_0 = 450\,\text{MPa}$ and a technical tensile strength of $\sigma_{c,\,tech} = R_m = 659\,\text{MPa}$. The technical uniform strain is defined as $\varepsilon_{c,tech} = A_g = 13.9\,\%$. The true maximum stress (saturation stress) converges to $\sigma_{a,true} = 900\,\text{MPa}$. A material designation such as HR450Y980T-DP is not sufficient to define the material behavior.

2.3 Data generation

The generation of training data was performed using the finite element program LS-DYNA by means of one-step-simulations. The meshes had about 10,000 shell elements with crash-typical element edge lengths of $3-5\,\text{mm}$. For this purpose, both generic geometries and real component geometries of the Toyota Yaris vehicle model were numerically investigated. In total, approximately 5,000 simulations were conducted to determine realistic areal strains $A_{r,real}$. The generic hardening curves used are shown in Fig. 5.

The training data cover a widely defined parameter space. The variation was systematically performed over physically consistent but deliberately generically chosen material parameters. This approach enables controlled and reproducible sampling of relevant material parameters without limiting to specific component or material configurations. In particular, the generic material modeling allows largely unbiased sampling of the parameter space, reducing systematic biases in the data basis for downstream AI models.

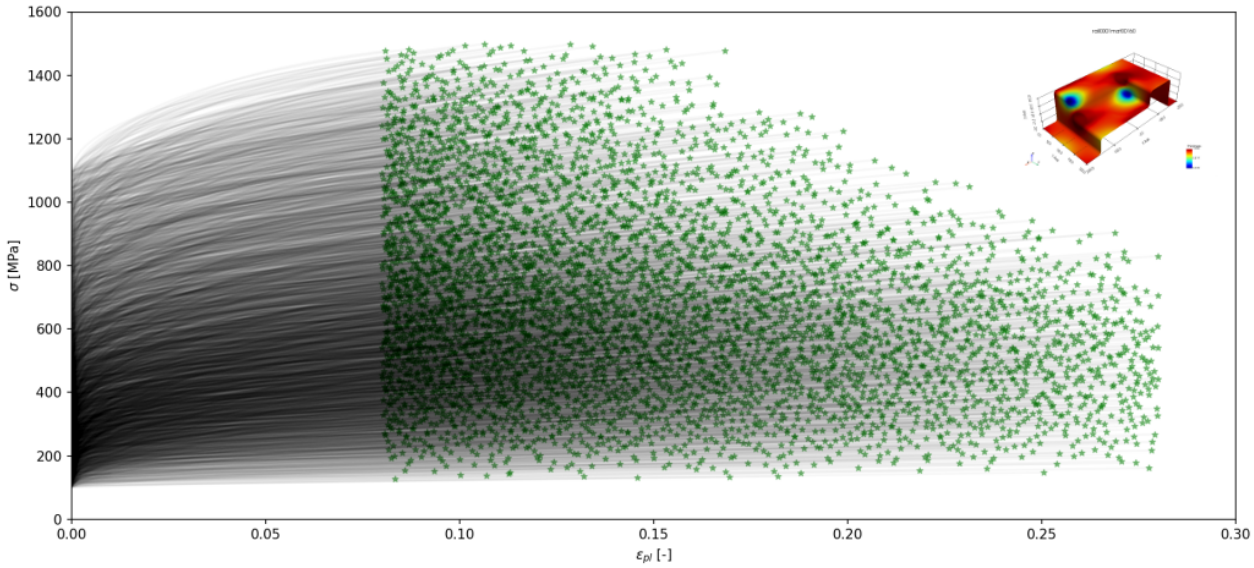

Fig. 5: Generic Hardening Curves

2.4 AI model

A monotonicity-preserving gradient boosting regressor is trained to map the five input parameters (areal strain $A_{\mathrm{r,\,uvmap}}$ and four Hockett–Sherby parameters σ_0, σ_c, σ_a, ε_c) to forming-induced target fields (areal strain $A_{\mathrm{r,\,real}}$, thickness t and plastic strains ε_pl), cf. the constraints in eqs 1-5.

$$A_{\mathrm{r,\,uvmap}} \propto A_{\mathrm{r,\,real}} \tag{1}$$

$$\sigma_0 \propto \varepsilon_\mathrm{pl} \tag{2}$$

$$\sigma_\mathrm{c} \propto \varepsilon_\mathrm{pl} \tag{3}$$

$$\sigma_\mathrm{a} \propto \varepsilon_\mathrm{pl} \tag{4}$$

$$\varepsilon_\mathrm{c} \propto 1/\varepsilon_\mathrm{pl} \tag{5}$$

Monotonicity constraints enforce physically plausible dependencies for constant material configurations and reduce unphysical extrapolation. Furthermore, during training, samples with pronounced

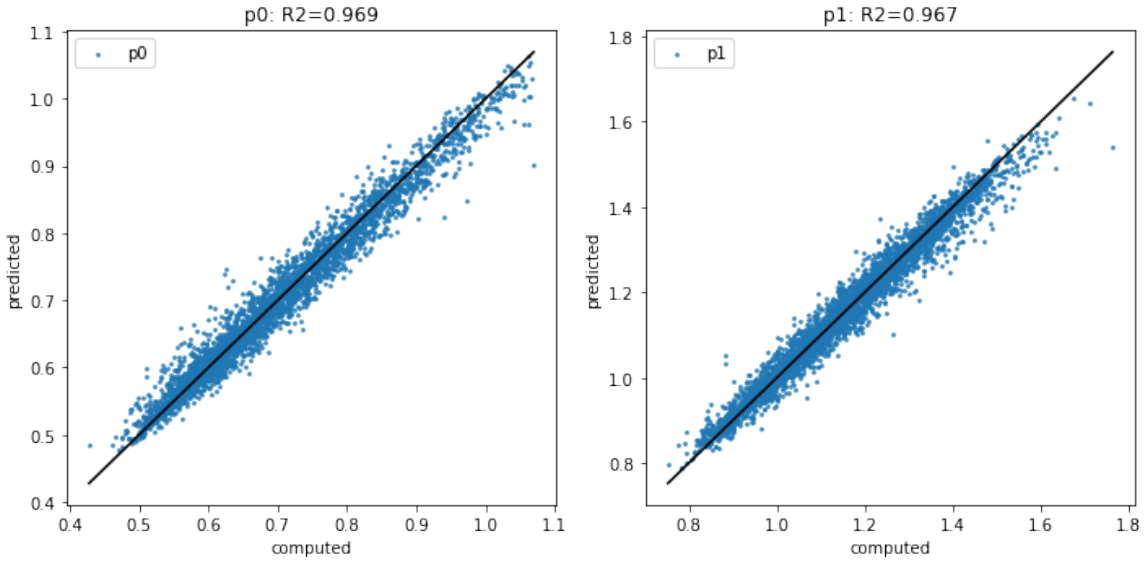

Fig. 6: Model accuracy of internal fit parameter p_1, p_2

thinning and large plastic strains are weighted higher to prioritize crash-relevant extrema while maintaining global approximation quality. This weighting does not reduce prediction quality for elements with low areal strain.

The mapping of the purely geometrically determined areal strains $A_{\mathrm{r,\,uvmap}}$ for each finite element to the simulated area strains $A_{\mathrm{r,\,real}}$ was carried out using equation 6. For each training data set with defined Hockett-Sherby material parameters, the model parameters p_0, p_1 were determined. These 5000 datasets (p0, p1) were used for training the UmMatCraML model.

$$A_{\mathrm{r,\,real}} = p_0\, e^{-p_1\, A_{\mathrm{r,\,uvmap}}} - 1 \tag{6}$$

Figure 6 shows all 5,000 simulation-based and predicted model parameters p_i. A perfect prediction would place all points on the diagonal. The results indicate a very high predictive accuracy with coefficients of determination $R^2 > 95\,\%$. This allows the material-dependent mapping from $A_{\mathrm{r,\,uvmap}}$ to $A_{\mathrm{r,\,real}}$ to be performed for each hardening law, cf. eq. 7.

$$A_{\mathrm{r,\,real}} = f(A_{\mathrm{r,\,uvmap}}, \sigma_0, \sigma_{\mathrm{c}}, \sigma_{\mathrm{a}}, \varepsilon_{\mathrm{c}}) \tag{7}$$

3. Verification and Validation

The verification of the proposed methodology addresses the correct implementation of the model assumptions and algorithms. It checks whether the model provides consistent and physically plausible predictions for manufacturing-induced sheet thickness distributions and plastic strains. Validation is performed through quantitative comparison of the results with established high-fidelity simulations (HFS) and low-fidelity simulations (LFS), which represent the state of the art in numerical forming simulation.

For the Kirchhoff Automotive demonstrator [7], HFS requires a computation time of about 60 min, while LFS is significantly faster at 10–15 min. The data-driven UmMatCraML model delivers comparable results in significantly less than 10 s. This results in an acceleration of the calculation of component properties by several orders of magnitude compared to HFS and at least one order of magnitude compared to LFS. This acceleration is achieved without explicit modeling of the deep drawing tools, which additionally reduces modeling effort, compare Fig. 7.

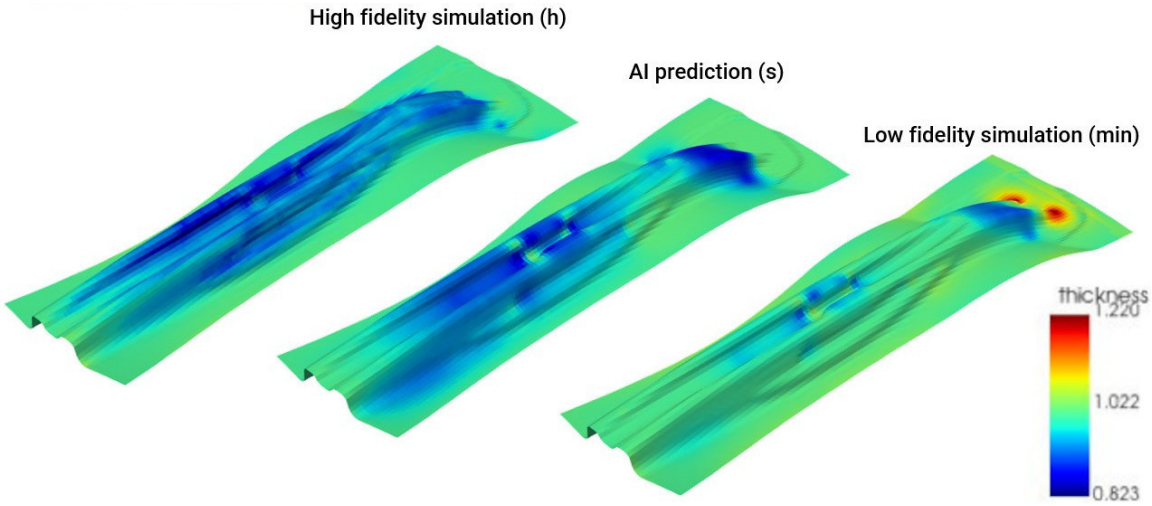

Fig. 7: Comparison of HFS, LFS, and the UmMatCraML Method for Kirchhoff Automotive Demonstrator Model – mild steel HS150Y273T284C450A – simulated vs. predicted element thicknesses $t = [0.823\,..\,1.220]$ mm

The prediction of crash-relevant minimum sheet thickness t_{min} for a mild steel confirms the accuracy of the approach, $t_{\mathrm{min,HFS}} = 0.82$ mm, $t_{\mathrm{min,LFS}} = 0.88$ mm, $t_{\mathrm{min,AI}} = 0.83$ mm.

For the Kirchhoff Automotive demonstrator [7], UmMatCraML predicts the maximum sheet thinning with an accuracy of about $0.1\,\mathrm{mm}$ compared to the high-fidelity reference solution $t_{\mathrm{min,HFS}}$, whereas the low-fidelity simulation (LFS) deviates by about $0.6\,\mathrm{mm}$ with respect to the minimum sheet thickness. In addition to the agreement of the extrema, the spatial thickness distributions show similar characteristics. The UmMatCraML model thus achieves accuracy close to HFS and surpasses LFS in both precision and computation time. Sheet thickening is also realistically predicted, compare Fig. 8.

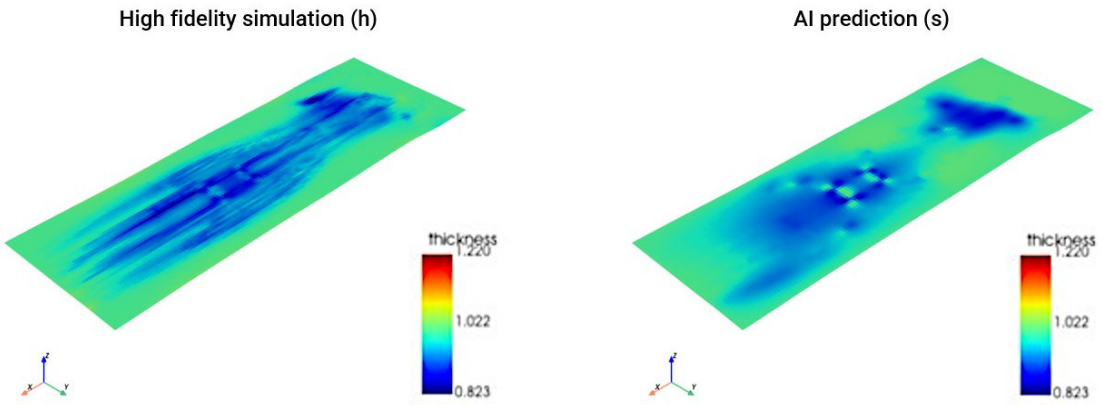

Fig. 8: Comparison of simulated and prediced Thicknesses (Projection on the Undeformed Sheet), $t_{\mathrm{min,\,HFS}} = [0.82\,..\,1.03]\,\mathrm{mm}$ vs. $t_{\mathrm{min,\,AI}} = [0.84\,..\,1.01]\,\mathrm{mm}$

The transferability of the method is investigated on the full-vehicle model of the Toyota Yaris. For geometrically and process-technically simple components, robust predictions of component properties are achieved.

Fig. 9 presents the model-based prediction of effective plastic strain in the B-pillar of the Toyota Yaris vehicle. The local quantification of plastic loading across the component geometry can be mapped. Areas of increased effective plastic strain mark zones with advanced plastic deformation and provide a direct indicator for potential failure or damage initiation.

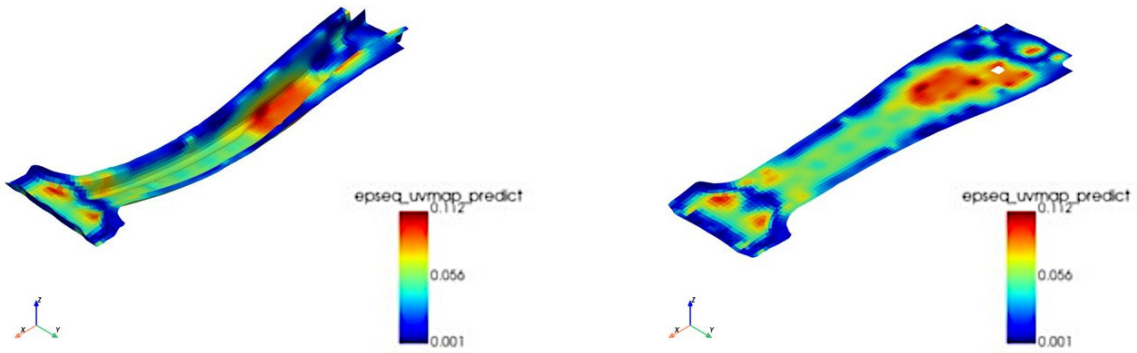

Fig. 9: Prediction Results of Plastic Strain $\varepsilon_{\mathrm{pl}} = [0\,..\,0.11]$ in the B-Pillar of the Toyota Yaris Vehicle.

Fig. 10 shows a component with pronounced trimming and several perforations. For this complex geometry, the UmMatCraML algorithm determines the required sheet blank with high accuracy. The results demonstrate that the algorithm provides robust estimates even with strongly reduced edge areas and structural openings. Under the model assumptions made, the method thus exhibits high potential for industrial application in early design and calculation phases.

Limitations appear in complex, multi-stage forming processes, where mapping process paths and intermediate steps requires increased model complexity. These results illustrate the potential of the

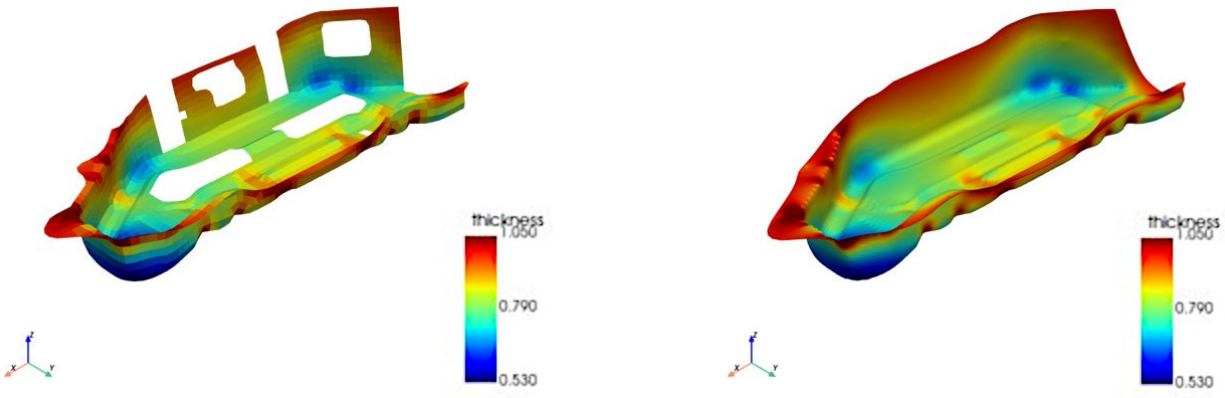

Fig. 10: Thickness Predictions $t = [0.53 \,..\, 1]$ mm for a Component with Strong Trimming and Openings

approach for efficient use in early development phases as well as the need for extended modeling for highly complex manufacturing chains.

Discussion. The presented results demonstrate the high prediction quality of UmMatCraML, with particular emphasis on real-time capability and geometric flexibility. For mild steels, sheet thicknesses are predicted with high agreement to high-fidelity simulations (HFS), and the deviation compared to low-fidelity simulations (LFS) is reduced from up to 0.06 mm to 0.01 mm. The monotonicity-preserving modeling approach addresses typical non-physical behavior of unconstrained regressors and enforces physically plausible dependencies for constant material configurations.

The methodology is subject to clearly defined assumptions. The modeling is restricted to isotropic, incompressible plastic material laws and J_2 plasticity, systematically excluding anisotropy and kinematic hardening. These simplifications are consistent with the early concept phase focus on dominant plastic deformations and sheet-thinning extrema, but they limit applicability for strongly anisotropic materials or process chains where detailed path effects become relevant.

Future work should expand the geometric input representation and improve robustness for complex trimming and perforation patterns. Further extensions include crack-risk prediction using load-state variables and the integration of additional quality indicators such as wrinkling and surface defects.

Conclusion and Outlook

UmMatCraML provides a reproducible medium-fidelity alternative to explicit forming simulation for early-phase concept crash assessments. It predicts forming-induced thickness and plastic strain fields directly on typical crash shell meshes without explicit tool modeling and reduces computation time from about 60 min (HFS) or 10–15 min (LFS) to under 10 s while improving accuracy compared to LFS under the stated assumptions. The method is coordinate-independent, handles trimmed and perforated geometries, and enables early integration of manufacturing-induced effects into crash models with low modeling effort.

Limitations arise from the deliberate restriction to isotropic hardening and one-step process abstraction. Within this scope, the approach closes the practical gap between fast but inaccurate LFS and accurate but expensive HFS and provides a robust basis for industrial applications such as concept crash simulation and, with additional boundary conditions and targets, blank optimization and tool-design support.

References

[1] Erman Tekkaya, A.: State-of-the-art of simulation of sheet metal forming, Journal of Materials Processing Technology, Volume 103, Issue 1, 2000, Pages 14-22

[2] Gassler, L.; Haberthür, M.; Afrasiabi, M.; Bambach, M.: Graph Neural Network-based Generation of Stamped Bipolar Plate Geometries from Tooling Surfaces. Journal of Physics: Conference Series 3104 (2025) 012059. IOP Publishing. DOI: 10.1088/1742-6596/3104/1/012059.

[3] Zhao, Y.; Chen, Q.; Li, H.; Zhou, H.; Attar, H. R.; Pfaff, T.: Recurrent U-Net- based Graph Neural Network (RUGNN) for accurate deformation predictions in sheet material forming. Advanced Engineering Informatics, Vol. 69, Part D, January 2026, Art.-Nr. 104021. ISSN 1474-0346. DOI: 10.1016/j.aei.2025.104021.

[4] Hockett, J.; Sherby, O.: Large strain deformation of polycrystalline metals at low homologous temperatures. Journal of the Mechanics and Physics of Solids 23(2), 87-98 (1975).

[5] SCALE.sdm - Integrative Software Solution for Continuous Simulation Data and Process, Management. https://www.scale.eu/en/products/scale-sdm/ (2025).

[6] Inal, K.; Lévesque, J., Worswick, M.: The 12th International Conference and Workshop on Numerical Simulation of 3D Sheet Metal Forming Processes (NUMISHEET 2022) (2022).

[7] Schwarzer, R.: Finite Element Model ”Kirchhoff-Automotive-Demonstrator” (KA-Demonstrator) - Process Model for Deep Drawing. KIRCHHOFF Automotive Deutschland GmbH (2025).

[8] Lepenies, I.; Krause, P.: Influence of Sheet Forming Using Machine Learning for Concept Crash Simulations. FAT Publication Series No. 395. Research Association for Automotive Engineering (FAT), Berlin 2025.

[9] 2010 Toyota Yaris Finite Element Model. https://www.ccsa.gmu.edu/models/2010-toyota-yaris/.

[10] Banabic, D.: Sheet Metal Forming Processes. Constitutive Modelling and Numerical Simulation.

[11] Roll, K.:Including the effect of manufacturing in the design of products: crash properties. Proc. Int. Conf. Product Property Prediction, Dortmund, 2010

[12] Zhu, X.; Zhang, L.: Advance in Sheet Metal Forming - One-step Solution, Multi-Beads, Gravity Prebending, Auto Nets, and Local Compensation 12th International LS-DYNA Users Conference, 2012, 12

[13] Güner, A.; Soyarslan, C.; Brosius, A.; Tekkaya, A. Characterization of anisotropy of sheet metals employing inhomogeneous strain fields for Yld2000-2D yield function International Journal of Solids and Structures , 2012, 49, 3517 - 3527

[14] Nielsen, C. V.; Martins, P. A.: Metal Forming: Formability, Simulation, and Tool Design Academic Press, 2021